Ferroelectrics, 483: 53–67, 2015

ISSN: 0015-0193 print / 1563-5112 online
DOI: 10.1080/00150193.2015.1058673

Taylor & Francis
Taylor & Francis Group

Comparative First-Principles Calculations of $SrTiO_3$, $BaTiO_3$, $PbTiO_3$ and $CaTiO_3$ (001), (011) and (111) Surfaces

ROBERTS I. EGLITIS*

Institute of Solid State Physics, University of Latvia, 8 Kengaraga Str., Riga LV 1063, Latvia

I present the results of my ab initio *calculations for $SrTiO_3$, $BaTiO_3$, $PbTiO_3$ and $CaTiO_3$ neutral (001), as well as for polar (011) and (111) surfaces using the hybrid description of exchange and correlation. AO and BO_2-terminations for the nonpolar (001) surface and A, BO, and O terminations of the polar (011) surface, as well as B and AO_3-terminations of the polar (111) surface were calculated. In the case of the neutral AO-terminated (001) surface for $SrTiO_3$, $BaTiO_3$, $PbTiO_3$ and $CaTiO_3$ perovskites, all upper-layer A atoms relax inward towards the bulk, while all second layer atoms relax outwards. For the BO_2-terminated (001) surface, in most cases, the largest relaxations are on the second-layer metal atoms. For practically all ABO_3 perovskites, the surface rumpling is considerably larger for the AO-terminated than for the BO_2-terminated (001) surface, but their surface energies always are almost equal. Just opposite, different terminations of the (011) ABO_3 surface lead to very different surface energies for the O-terminated, A-terminated, and BO-terminated (011) surface, respectively. The surface energies for all calculated (111) surfaces are considerably larger than even for (011) surfaces. A considerable increase in the Ti-O chemical bond covalency near the (011) surface as compared to the bulk and to the (111) and (001) surfaces in considered ABO_3 perovskites were predicted.*

Keywords $SrTiO_3$; $BaTiO_3$; $PbTiO_3$; $CaTiO_3$; (001); (011) and (111) surfaces

Introduction

ABO_3 perovskites are important for a variety of high technology applications as a result of their diverse physical properties [1–4]. Thin films of oxide perovskite ferroelectrics are important for many emerging industrial applications including high capacity memory cells, catalysis, optical wave guides, integrated optics applications, substrates for high-T_c cuprate superconductor growth, etc. [5]. For all these applications, the surface structure and the related surface electronic and physical properties are of great importance. Ab initio calculations of $SrTiO_3$, $BaTiO_3$, $PbTiO_3$ and $CaTiO_3$ surface characteristics are useful to understand processes in which surfaces play a crucial role, such as the chemistry of surface reactions, interface phenomena, and adsorption. In this study, my theoretical calculations dealing with relaxed atomic structures of the $SrTiO_3$, $BaTiO_3$, $PbTiO_3$ and $CaTiO_3$

Received October 2, 2014; in final form April 14, 2015.
*Corresponding author. E-mail: rieglitis@gmail.com
Color versions of one or more figures in this article can be found online at www.tandfonline.com/gfer.

(001), (011) and (111) surfaces are reported, and general, characteristic trends for all four materials are analyzed.

Due to intensive development and progressive miniaturization of electronic devices, the surface structure as well as the electronic properties of the ABO_3 perovskite thin (001) films have been extensively studied experimentally in recent years. On the (011) surfaces considerably less experimental studies were performed. For example, Enterkin *et al*. [6] recently reported a solution to the 3×1 $SrTiO_3$ (110) surface structure obtained through transmission electron diffraction, and confirmed through density functional theory calculations and scanning tunneling microscopy images and simulations [6]. There exist several experimental studies dealing with $SrTiO_3$ (111) surfaces. For example, Tanaka and Kawai have obtained clean surfaces of reduced $SrTiO_3$ (111) crystals and observed them by means of scanning tunneling microscopy (STM) combined with reflection high energy diffraction. They have observed two different surface structures. One obtained by annealing at the temperature $\sim$ 1.180°C, is assigned to have a SrO_3 outermost layer. The other, obtained by annealing at the temperature˜1.220°C, is assigned to have a Ti outermost layer [7]. More than 10 years later Chang *et al*. [8] also reproducibly obtained an atomically well-defined $SrTiO_3$ (111) surface by a combined chemical etching and thermal annealing process.

It is obvious, that the high technological importance of $SrTiO_3$, $BaTiO_3$, $PbTiO_3$ and $CaTiO_3$ perovskites has motivated several *ab initio* studies of their (001) surfaces [9–20]. ABO_3 perovskite (011) surfaces, in general, and $SrTiO_3$ (011) surfaces, in particular, are considerably less well studied than the corresponding (001) surfaces. Due to the very complex polar structure, only very few ab initio studies of ABO_3 perovskite (011) surfaces exist [21–27]. ABO_3 perovskite polar (111) surfaces, on the theory side, are even less studied than their (011) surfaces [28–32]. In order to fill this gap, in this study I report comprehensive results dealing with $SrTiO_3$, $BaTiO_3$, $PbTiO_3$ and $CaTiO_3$ (001), (011) and (111) surface atomic and electronic structures.

Ferroelectrics 2015.483:53-67.

Computational Details

First-principles calculations in the framework of density-functional theory (DFT) using the CRYSTAL computer code[111] have been carried out. Unlike the plane-wave codes employed in many previous studies, CRYSTAL uses localized Gaussian-type basis sets. In calculations by Piskunov *et al*. [33], the basis sets (BS) were developed for $SrTiO_3$, $BaTiO_3$ and $PbTiO_3$. In this paper, for most of calculations, for O atoms, this new BS which differs from previous calculations [10, 11] by inclusion of polarizable d-orbitals on O ions were used. Most of calculations in this paper were performed using the hybrid exchange-correlation B3PW functional involving a mixture of nonlocal Fock exact exchange, local-density approximation (LDA) exchange, and Becke's gradient corrected exchange functional, [34] combined with the nonlocal gradient corrected correlation potential of Perdew and Wang [35–37]. The hybrid B3PW functional for most of ABO_3 perovskite surface studies were selected because it yields excellent results for the $SrTiO_3$, $BaTiO_3$, and $PbTiO_3$ bulk lattice constant and bulk modulus [33].

The reciprocal-space integration was performed by sampling the Brillouin zone, in most cases, with an $8 \times 8 \times 8$ Pack-Monkhorst mesh [38] which provides a balanced summation in direct and reciprocal spaces. To achieve high accuracy, large enough tolerances of 7, 8, 7, 7, and 14 were chosen for the dimensionless Coulomb overlap, Coulomb penetration, exchange overlap, first exchange pseudo-overlap, and second exchange pseudo-overlap parameters, respectively [39]. An advantage of the CRYSTAL code is

that it treats isolated two-dimensional slabs, without any artificial periodicity in the z direction perpendicular to the surface.

The $SrTiO_3$ (001) surfaces were modeled using symmetric (with respect to the mirror plane) slabs consisting of seven alternating TiO_2 and SrO layers, respectively. (Henceforth, $SrTiO_3$ will be used for presentation purposes, but everything that is said will apply equally to the $BaTiO_3$, $PbTiO_3$ and $CaTiO_3$ cases). One of these slabs was terminated by SrO planes for the $SrTiO_3$ crystal and consisted of a supercell containing 17 atoms. The second slab was terminated by TiO_2 planes and consisted of a supercell containing 18 atoms. These slabs are nonstoichiometric, with unit cell formulas $Sr_4Ti_3O_{10}$ and $Sr_3Ti_4O_{11}$ for the $SrTiO_3$ perovskite. These two (SrO and TiO_2) terminations are the only two possible flat and dense (001) surfaces for the $SrTiO_3$ perovskite lattice structure. The sequence of layers with definition of surface rumpling s and the near-surface interplanar separations Δd_{12} and Δd_{23} at the TiO_2-terminated (001) surface of $SrTiO_3$ is illustrated in Fig. 1.

Unlike the (001) cleavage of $SrTiO_3$, which naturally gives rise to nonpolar SrO and TiO_2 terminations, a naive cleavage of $SrTiO_3$ to create (011) surfaces leads to the formation of polar surfaces. For example, the stacking of the $SrTiO_3$ crystal along the [011] direction consists of alternating planes of O_2 and SrTiO units having nominal charges of $-4e$ and $+4e$, respectively, assuming O^{2-}, Ti^{4+}, and Sr^{2+} constituents. Thus, a simple cleavage leads to O_2-terminated and SrTiO-terminated (011) surfaces that are *polar* and have nominal surface charges of $-2e$ and $+2e$ per surface cell, respectively. These are shown as the top and bottom surfaces in Fig. 2(a), respectively. If uncompensated, the surface charge would lead to an infinite electrostatic cleavage energy. In reality, the polar surfaces would probably become metallic in order to remain neutral, but in view of the large electronic gaps in the perovskites, such metallic surfaces would presumably be unfavorable. Thus, we may expect rather generally that such polar crystal terminations are relatively unstable in this class of materials.

On the other hand, if the cleavage occurs in such a way as to leave a half layer of O_2 units on each surface, we obtain the nonpolar surface structure shown in Fig. 2(b). Every other surface O atom has been removed, and the remaining O atoms occupy the same sites

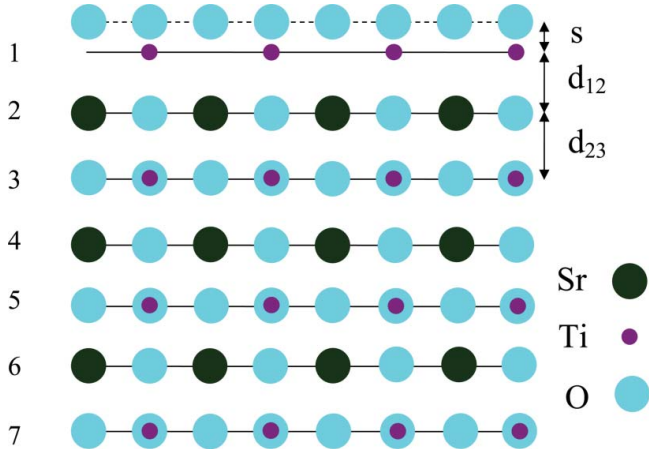

Figure 1. TiO_2-terminated $SrTiO_3$ (001) surface with definitions of surface rumpling s and the near-surface interplanar separations Δd_{12} and Δd_{23}.

Ferroelectrics 2015.483:53-67.

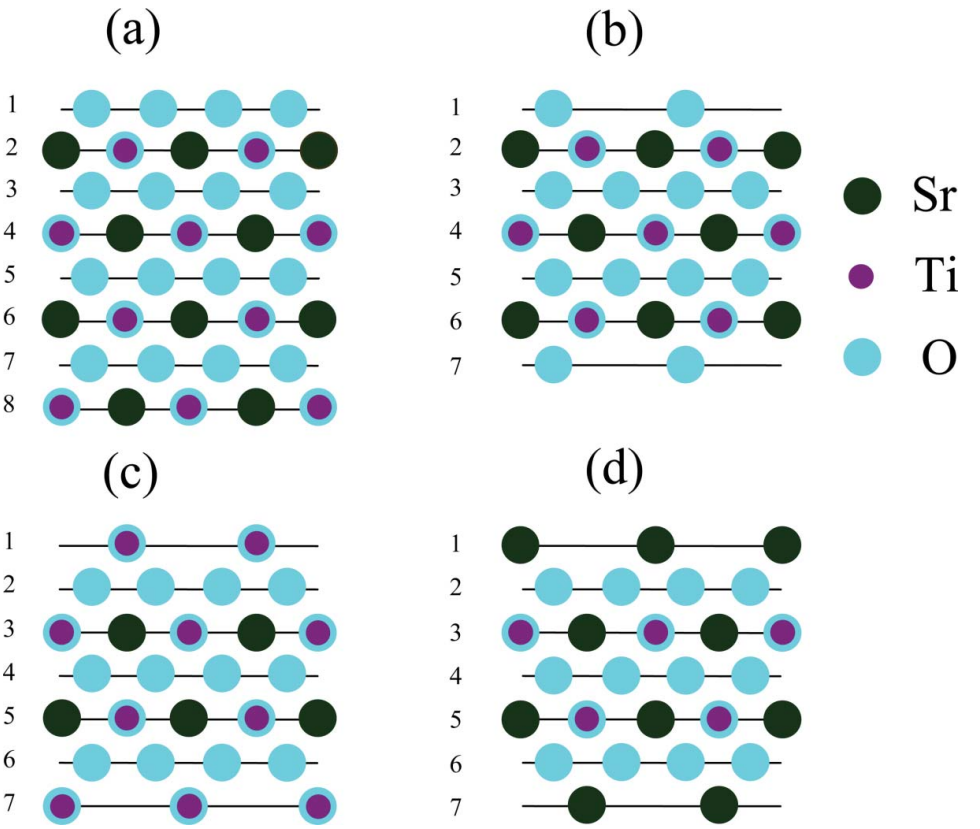

Figure 2. Side views of slab geometries used to study $SrTiO_3$ (011) surfaces. (a) Stoichiometric eight-layer slab with O_2-terminated and SrTiO-terminated surfaces at top and bottom, respectively. (b) Seven-layer slab with O-terminated surfaces. (c) Seven-layer slab with TiO-terminated surfaces. (d) Seven-layer slab with Sr-terminated surfaces.

Ferroelectrics 2015.483:53-67.

as in the bulk structure. We shall refer to this as the "O-terminated" (011) surface, in distinction to the "O_2-terminated" polar surface already discussed in Fig. 2(a). The nonpolar nature of the O-terminated surface can be confirmed by nothing that the 7-layer 15-atom $Sr_3Ti_3O_9$ slab shown in Fig. 2(b), which has two O-terminated surfaces, is neutral. It is also possible to make nonpolar TiO-terminated and Sr-terminated surfaces, as shown in Figs. 2(c) and 2(d), respectively. This is accomplished by splitting a SrTiO layer during cleavage, instead of splitting an O_2 layer. For the TiO- and Sr-terminated surfaces, we use seven-layer slabs having composition $Sr_2Ti_4O_{10}$ (16 atoms) and $Sr_4Ti_2O_8$ (14 atoms) as shown in Figs. 2(c) and 2(d), respectively. These are again neutral, showing that the surfaces are nonpolar (even though they no longer have precisely the bulk $SrTiO_3$ stoichiometry).

As a next step, the ABO_3 perovskite (111) surfaces will be discussed on the example of $BaZrO_3$. To simulate $BaZrO_3$ (111) surfaces, symmetrical slabs consisting of nine alternating Zr and BaO_3 layers were used (see Fig. 3). One of these slabs is terminated by Zr planes and consists of a supercell containing 21 atoms (Zr-BaO_3-Zr-BaO_3-Zr-BaO_3-Zr-BaO_3-Zr) (see Fig. 4a). The second slab is terminated by BaO_3 planes and consists of a supercell containing 24 atoms (BaO_3-Zr-BaO_3-Zr-BaO_3-Zr-BaO_3-Zr-BaO_3) (see

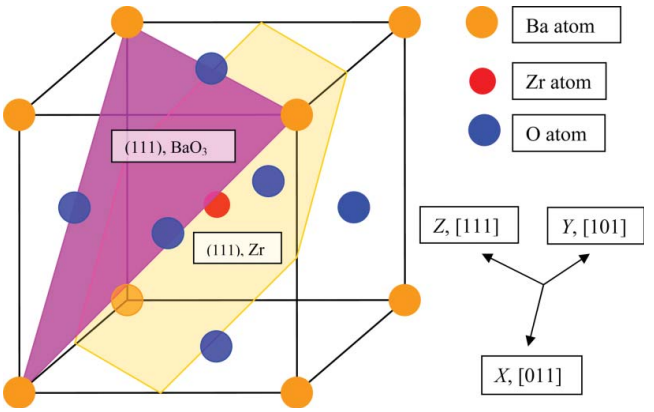

Figure 3. Sketch of the cubic $BaZrO_3$ perovskite structure showing two possible (111) surface terminations: BaO_3 and Zr.

Fig. 4b). These slabs are non-stoichiometric, with unit cell formulas $Ba_4Zr_5O_{12}$ and $Ba_5Zr_4O_{15}$, respectively (see Fig. 3). As it is well known from previous studies dealing with polar $CaTiO_3$ and $SrTiO_3$ (111) surfaces [30, 40, 41], a strong electron redistribution takes place for such terminations in order to cancel the polarity, but the Zr or BaO_3-

Ferroelectrics 2015.483:53-67.

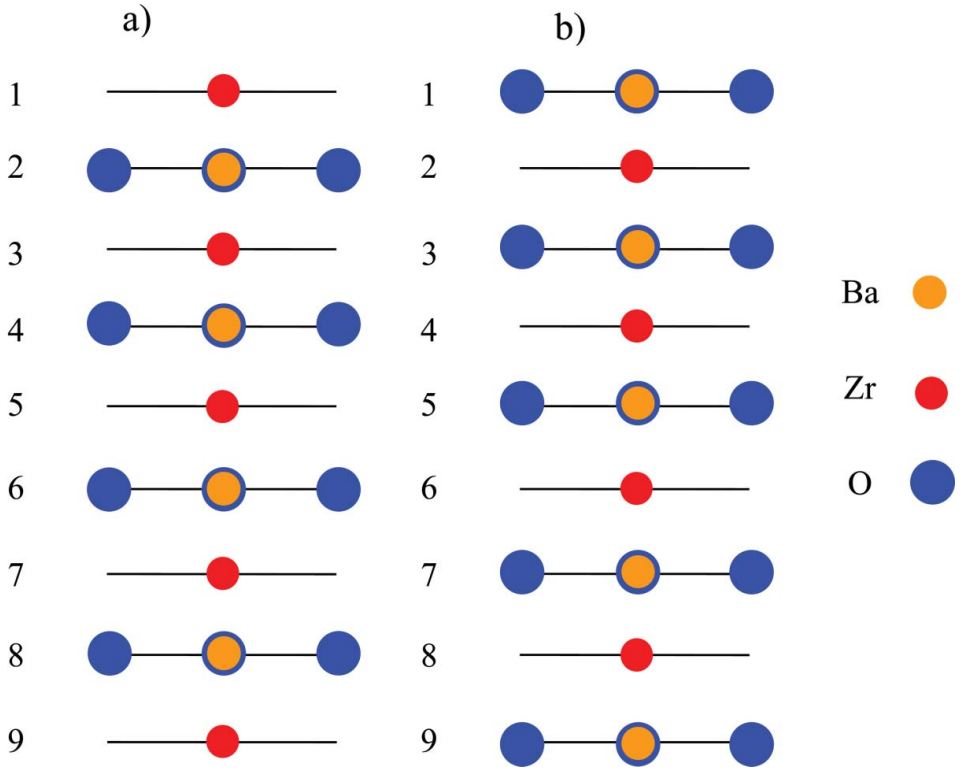

Figure 4. Sketch of the side views of slab geometries used to study $BaZrO_3$ (111) surfaces. (a) Non-stoichiometric nine-layer slab with Zr-terminated surfaces. (b) Non-stoichiometric nine-layer slab with BaO_3-terminated surfaces.

terminated $BaZrO_3$ (111) surface keeps its insulating character, and such calculations are feasible. Of course, it is not possible to perform calculations for asymmetric slabs with different terminations, for example, Zr-BaO_3-Zr-BaO_3-Zr-BaO_3-Zr-BaO_3, since this would lead to a large dipole moment for an asymmetric slab.

In order to calculate ABO_3 perovskite, for example, the $SrZrO_3$ (001) surface energy, I started with the cleavage energy for unrelaxed SrO- and ZrO_2-terminated (001) surfaces. Surfaces with both terminations simultaneously arise under (001) cleavage of the crystal, and I adopt the convention that the cleavage energy is equally distributed between the created surfaces. In my calculations, the nine-layer SrO-terminated (001) slab with 22 atoms and the ZrO_2-terminated one with 23 atoms represent, together, nine bulk unit cells (45 atoms) so that

$$E_{surf}^{unr}(\Omega) = {}^{1}\!/_{4}\left[E_{slab}^{unr}(SrO) + E_{slab}^{unr}(ZrO_2) - 9E_{bulk}\right], \tag{1}$$

where Ω denotes SrO or ZrO_2, $E_{\mathrm{slab}}^{\mathrm{unr}}(\Omega)$ are the unrelaxed energies of the SrO- or ZrO_2-terminated (001) slabs, E_{bulk} is the energy per bulk unit cell, and the factor of ¼ comes from the fact that I create four surfaces upon the crystal cleavage procedure. Next, I can calculate the relaxation energies for each of SrO and ZrO_2 terminations, when both sides of the slabs relax, according to

$$E_{rel}(\Omega) = {}^{1}\!/_{2}\left[E_{slab}^{rel}(\Omega) - E_{slab}^{unr}(\Omega)\right], \tag{2}$$

where $E_{\mathrm{slab}}^{\mathrm{rel}}(\Omega)$ is the slab energy after relaxation (and again Ω = SrO or ZrO_2). The surface energy is then defined as a sum of the cleavage and relaxation energies,

$$E_{surf}(\Omega) = E_{surf}^{unr}(\Omega) + E_{rel}(\Omega). \tag{3}$$

In order to calculate the $SrZrO_3$ (011) surface energies for the ZrO- and Sr-terminated surfaces, I consider the cleavage of eight bulk unit cells (40 atoms) to result in the ZrO- and Sr-terminated slabs, containing 21 and 19 atoms, respectively. I again divide the cleavage energy equally between these two surfaces and obtain

$$E_{surf}^{unr}(\Omega) = {}^{1}\!/_{4}\left[E_{slab}^{unr}(Sr) + E_{slab}^{unr}(ZrO) - 8E_{bulk}\right], \tag{4}$$

where Ω denotes Sr or ZrO, $E_{\mathrm{slab}}^{\mathrm{unr}}(\Omega)$ is the energy of the unrelaxed Sr- or ZrO-terminated (011) slab, and E_{bulk} is the $SrZrO_3$ energy per bulk unit cell.

Finally, when I cleave the $SrZrO_3$ crystal in another way, I obtain two identical O-terminated (011) surface slabs containing 20 atoms each. This allows for me to simplify the calculations since the unit cell of the nine-plane O-terminated (011) slab contains four bulk unit cells. Therefore, the relevant surface energy is

$$E_{surf}(O) = {}^{1}\!/_{2}\left[E_{slab}^{rel}(O) - 4E_{bulk}\right], \tag{5}$$

where $E_{\mathrm{surf}}(\mathrm{O})$ and $E_{\mathrm{slab}}^{\mathrm{rel}}(\mathrm{O})$ are the surface energy and the relaxed slab total energy for the O-terminated (011) surface. The ABO_3 perovskite polar (111) surface energy calculations, using as an example the $BaZrO_3$ crystal, were discussed in Ref. 31.

Ferroelectrics 2015.483:53-67.

Table 1
The calculated bulk lattice constants (in Å) for the $SrTiO_3$, $BaTiO_3$, $PbTiO_3$ and $CaTiO_3$ bulk using the hybrid B3PW method. The experimental bulk lattice constants [42–44] are listed for comparison

Crystal	B3PW	Experiment
$SrTiO_3$	3.904	3.89 [42]
$BaTiO_3$	4.008	4.00 [42]
$PbTiO_3$	3.936	3.97 [43]
$CaTiO_3$	3.851	3.895 [44]

Main Calculation Results

As a first step of my calculations, I calculated the $SrTiO_3$, $BaTiO_3$, $PbTiO_3$ and $CaTiO_3$ bulk lattice constants using the hybrid B3PW functional (see Table 1). The experimentally measured $SrTiO_3$, $BaTiO_3$, $PbTiO_3$ and $CaTiO_3$ bulk lattice constants [42–44] are listed for comparison purposes in Table 1. The B3PW calculated bulk lattice constants for $SrTiO_3$ and $BaTiO_3$ crystals are almost in perfect agreement with experiments [42], but my calculation results for $PbTiO_3$ and $CaTiO_3$ are slightly smaller than the experimental values [43, 44].

My calculation results for the surface atomic displacements for SrO, BaO, PbO, CaO and TiO_2-terminated $SrTiO_3$, $BaTiO_3$, $PbTiO_3$ and $CaTiO_3$ perovskite upper two (001) surface layers are listed in Tables 2 and 3. The relaxation of surface metal atoms for $SrTiO_3$, $BaTiO_3$, $PbTiO_3$ and $CaTiO_3$ perovskite upper two surface layers for both (001) terminations – AO and TiO_2 are much larger than that of oxygen ions what leads to a leads to a considerable rumpling of the outermost plane (see Tables 2, 3 and 4). For the AO-terminated $SrTiO_3$, $BaTiO_3$, $PbTiO_3$ and $CaTiO_3$ (001) surface, the atoms of the first surface layer relax inwards, whereas the all atoms of the second surface layer relax outwards. The only exception is the upwards relaxation of the oxygen atom located on the first layer of SrO-terminated $SrTiO_3$ (001) surface (see Table 2).

The CaO-terminated $CaTiO_3$ (001) surface first layer Ca atoms exhibit the strongest relaxation between all AO and TiO_2-terminated ABO_3 perovskite (001) surface atoms.

Table 2
Calculated atomic relaxation (in percent of bulk lattice constant) for SrO, BaO, PbO and CaO-terminated $SrTiO_3$, $BaTiO_3$, $PbTiO_3$ and $CaTiO_3$ (001) surfaces, respectively. Positive (negative) values refer to displacements outward from (inward to) the surface

SrO-termin. $SrTiO_3$ (001) surf.			BaO-term. BTO (001)		PbO-term PTO (001)		CaO-term CTO (001)	
Layer	Ion	B3PW	Ion	B3PW	Ion	B3PW	Ion	B3PW
1	Sr	−4.84	Ba	−1.99	Pb	−3.82	Ca	−8.31
	O	0.84	O	−0.63	O	−0.31	O	−0.42
2	Ti	1.75	Ti	1.74	Ti	3.07	Ti	1.12
	O	0.77	O	1.40	O	2.30	O	0.01

Ferroelectrics 2015.483:53-67.

Table 3
Calculated atomic relaxation (in percent of bulk lattice constant) for TiO_2-terminated $SrTiO_3$, $BaTiO_3$, $PbTiO_3$ and $CaTiO_3$ (001) surfaces, respectively. Positive (negative) values refer to displacements outward from (inward to) the surface

TiO_2-termin. $SrTiO_3$ (001) surf.			TiO_2-term. BTO (001)		TiO_2-term PTO (001)		TiO_2-term CTO (001)	
Layer	Ion	B3PW	Ion	B3PW	Ion	B3PW	Ion	B3PW
1	Ti	−2.25	Ti	−3.08	Ti	−2.81	Ti	−1.71
	O	−0.13	O	−0.35	O	0.31	O	−0.10
2	Sr	3.55	Ba	2.51	Pb	5.32	Ca	2.75
	O	0.57	O	0.38	O	1.28	O	1.05

The Ca atom inward relaxation magnitude is 8.31% of the theoretically by B3PW calculated $CaTiO_3$ lattice constant.

In order to compare the calculated surface structures with experimental results, the surface rumpling s (the relative displacement of oxygen with respect to the metal atom in the surface layer) and the changes in interlayer distances Δd_{12} and Δd_{23} (1, 2 and 3 are the numbers of near-surface layers) are presented in Table 4. According to my B3PW calculations, the amplitude of surface rumpling of SrO-terminated $SrTiO_3$ (001) surface is predicted to be much larger than that of TiO_2-terminated $SrTiO_3$ surface, whereas the rumpling of $BaTiO_3$ TiO_2-terminated (001) surface is predicted to exceed by a factor of two that for BaO-terminated $BaTiO_3$ (001) surface. In contrast, the $PbTiO_3$ perovskite demonstrates practically equal surface rumpling for both PbO and TiO_2 (001) surface terminations. From Table 4, one can see that all calculated surfaces show the reduction of the interlayer distance d_{12} and expansion of d_{23}. The only exception is PbO-terminated $PbTiO_3$ (001) surface, which shows the expansion between the first and second surface layer.

My calculated surface energy for the SrO-terminated $SrTiO_3$ (001) surface by means of the hybrid B3PW method is 1.15 eV, which is slightly smaller than the

Table 4
Calculated and experimental surface rumpling s and relative displacements of the three near-surface planes for the AO and TiO_2-terminated $SrTiO_3$, $BaTiO_3$, $PbTiO_3$ and $CaTiO_3$ (001) surfaces Δd_{ij} (in percent of the lattice constant)

		AO-terminated			TiO_2-terminated		
Crystal	Method	s	Δd_{12}	Δd_{23}	s	Δd_{12}	Δd_{23}
$SrTiO_3$	B3PW	5.66	−6.58	1.75	2.12	−5.79	3.55
	LEED [45]	4.1 ± 2	−5 ± 1	2 ± 1	2.1 ± 2	1 ± 1	−1 ± 1
	RHEED [46]	4.1	2.6	1.3	2.6	1.8	1.3
$BaTiO_3$	B3PW	1.37	−3.74	1.74	2.73	−5.59	2.51
$PbTiO_3$	B3PW	3.51	6.89	3.07	3.12	−8.13	5.32
$CaTiO_3$	B3PW	7.89	−9.43	1.12	1.61	−4.46	2.75

Ferroelectrics 2015.483:53-67.

Table 5
My calculated surface energies (in eV per surface cell) for $SrTiO_3$, $BaTiO_3$, $PbTiO_3$ and $CaTiO_3$ (001), (011) and (111) surfaces with different terminations

Crystal	(001)		(011)			(111)	
Terminat.	AO	BO_2	BO	A	O	AO_3	B
$SrTiO_3$	1.15	1.23	3.06	2.66	2.04	6.30	4.99
$BaTiO_3$	1.19	1.07	2.04	3.24	1.72	8.40	7.28
$PbTiO_3$	0.83	0.74	1.36	2.03	1.72		
$CaTiO_3$	0.94	1.13	3.13	1.91	1.86	5.86	4.18

computed surface energy of 1.23 eV for the TiO_2-terminated $SrTiO_3$ (001) surface (see Table 5). Just opposite to the $SrTiO_3$ (001) surface, the different terminations of the (011) surface lead to large differences in the surface energies. For the $SrTiO_3$ (011) surface, the lowest energy, according to my B3PW calculations is 2.04 eV for the O-terminated surface. The calculated surface energy of 3.06 eV for the TiO-terminated $SrTiO_3$ (011) surface is larger than that of the Sr-terminated (011) surface (2.66 eV). The B3LYP calculated surface energy for the Ti-terminated $SrTiO_3$ (111) surface (4.99 eV) is smaller, than the surface energy for SrO_3-terminated $SrTiO_3$ (111) surface (6.30 eV). My calculated surface energies of the relaxed $BaTiO_3$ (001) and (011) surfaces by means of the hybrid B3PW method are presented in Table 5. The calculated energies for BaO and TiO_2-terminated $BaTiO_3$ (001) surfaces (1.19 eV and 1.07 eV, respectively) demonstrate only a small difference. According to my calculations performed by the hybrid B3PW method, unlike the $BaTiO_3$ (001) surface, different terminations of the $BaTiO_3$ (011) surface show great differences in the surface energies. The lowest surface energy has the O-terminated $BaTiO_3$ (011) surface (1.72 eV). The Ba-terminated $BaTiO_3$ (011) surface shows much higher surface energy of 3.24 eV, while the $BaTiO_3$ TiO-terminated (011) surface energy is 2.04 eV. Similarly as for the $SrTiO_3$ perovskite, also for $BaTiO_3$, the (111) surface energies are considerably larger than the (001), and even (011) surface energies. My B3LYP calculated surface energy for Ti-terminated $BaTiO_3$ (111) surface is equal to 7.28 eV, while the surface energy for BaO_3-terminated $BaTiO_3$ (111) surface is equal to 8.40 eV.

Table 6 for the $SrTiO_3$, $BaTiO_3$, $PbTiO_3$ and $CaTiO_3$ (011) surfaces is similar to Table 3 for the corresponding (001) surfaces, whereas Table 7 complements these data by the predicted (011) surface rumpling and the relative displacements of the two top layers. For the TiO-terminated (011) surface, the rumpling for all four $SrTiO_3$, $BaTiO_3$, $PbTiO_3$ and $CaTiO_3$ surfaces is qualitatively equal and really huge, $\approx 10 - 12$ % of the bulk lattice constant. For all four calculated ABO_3 perovskites, this arise due to a combination of a strong O ion outward displacement by (2–5%) and large Ti ion inward displacement by approximately (7–8%). This calculated surface rumpling is considerably larger than that found for the $SrTiO_3$, $BaTiO_3$, $PbTiO_3$ and $CaTiO_3$ (001) surface. The reduction of relative distances between the first and second layer for TiO-terminated (011) surfaces for all four my calculated ABO_3 perovskites (see Table 7) are in the range between (4%) and (7%). This reduction of the interlayer distance between the first and the second layer is considerably larger than the reduction of the interlayer distance between the second and the third layer. As we can wee from the Table 7, the TiO-terminated $CaTiO_3$ (011) surface, in contrast to the $SrTiO_3$, $BaTiO_3$ and $PbTiO_3$ perovskites, shows expansion between the second and third layers by (2.31%) of the bulk lattice constant.

Ferroelectrics 2015.483:53-67.

Table 6
Atomic relaxation of the $SrTiO_3$, $BaTiO_3$, $PbTiO_3$ and $CaTiO_3$ (011) surfaces (in percent of the bulk lattice constant) for the three terminations calculated by means of the *ab initio* B3PW method

	$SrTiO_3$			$BaTiO_3$			$PbTiO_3$			$CaTiO_3$		
Layer	Ion	Δz	Δy	Ion	Δz	Δy	Ion	Δz	Δy	Ion	Δz	Δy
	TiO-terminated (011) surface				TiO-term. (011) surf.			TiO-term. (011) surf.			TiO-term. (011) surf.	
1	Ti	−7.69	—	Ti	−7.86	—	Ti	−8.13	—	Ti	−7.14	—
	O	3.59	—	O	2.61	—	O	3.30	—	O	4.67	—
2	O	−0.51	—	O	−1.02	—	O	−0.41	—	O	−0.44	—
3	Sr	−2.10	—	Ba	−0.88	—	Pb	−2.54	—	Ca	−2.75	—
	O	−2.56	—				O	−4.07	—	O	−3.79	—
	Ti	0.16	—				Ti	0.30	—	Ti	−0.78	—
	Sr-terminated (011) surface				Ba-term. (011) surf.			Pb-term. (011) surf.			Ca-term. (011) surf.	
1	Sr	−12.81	—	Ba	−8.67	—	Pb	−11.94	—	Ca	−16.05	—
2	O	1.02	—	O	0.80	—	O	−0.61	—	O	1.35	—
3	Ti	−0.04	—	Ti	0.16	—	Ti	1.78	—	Ti	−0.37	—
	O	−1.08	—	O	−0.43	—	O	1.67	—	O	−1.71	—
	Sr	0.26	—				Pb	1.52	—	Ca	−0.93	—
	O-terminated (011) surface				O-term. (011) surf.			O-term. (011) surf.			O-term. (011) surf.	
1	O	−6.61	−0.14	O	−5.40	−1.67	O	−7.37	−0.07	O	−6.10	−2.16
2	Ti	−1.02	−4.35	Ti	−0.15	−6.38	Ti	0.20	−2.54	Ti	−0.26	−4.70
	Sr	−1.18	0.85	Ba	1.54	−1.27	Pb	0.18	−7.50	Ca	−2.10	−0.27
	O	1.79	6.40	O	1.95	2.97	O	0.51	2.19	O	3.43	8.05
3	O	−0.79	2.10	O	0.90	4.49	O	−0.41	3.30	O	−0.55	1.90

On the Sr, Ba, Pb and Ca-terminated $SrTiO_3$, $BaTiO_3$, $PbTiO_3$ and $CaTiO_3$ (011) surfaces, the upper layer Sr, Ba, Pb and Ca atoms move very strongly inwards by 12.81, 8.67, 11.94 and 16.05% of the lattice constant a_0, respectively (see Table 6). These Sr, Ba, Pb and Ca atomic displacement magnitudes are the largest atomic displacement

Table 7
Surface rumpling s and relative displacements Δd_{ij} (in percent of the bulk lattice constant) for three near-surface planes of the TiO and O-terminated $SrTiO_3$, $BaTiO_3$, $PbTiO_3$ and $CaTiO_3$ (011) surface

	TiO-terminated (011) surface			O-terminated (011) surface	
Crystal	s	Δd_{12}	Δd_{23}	Δd_{12}	Δd_{23}
$SrTiO_3$	11.28	−7.18	−0.67	−5.59	−0.23
$BaTiO_3$	10.47	−6.84	−1.02	−5.25	−1.05
$PbTiO_3$	11.43	−4.83	−0.71	−7.57	−5.84
$CaTiO_3$	11.81	−6.70	2.31	−5.84	0.29

Ferroelectrics 2015.483:53-67.

magnitudes between all in the Table 6 calculated $SrTiO_3$, $BaTiO_3$, $PbTiO_3$ and $CaTiO_3$ (011) surface atoms. The second layer O atoms for the Sr, Ba and Ca-terminated $SrTiO_3$, $BaTiO_3$ and $CaTiO_3$ (011) surfaces relax outwards by 1.02, 0.80 and 1.35% of a_0, respectively, whereas the Pb-terminated $PbTiO_3$ (011) surface second layer O atom, in contrast, relax inwards by 0.61% of a_0 (see Table 6). For the O-terminated $SrTiO_3$, $BaTiO_3$, $CaTiO_3$ and $PbTiO_3$ (011) surface (see Table 6), the upper layer O atom displacement directions along the z- and y-axes are the same for all four calculated perovskites. Nevertheless, the displacement magnitudes of the upper layer O atom are quite different for different perovskites. As we can see from Table 6, the atomic displacement magnitudes in the third plane from the surface for all three terminations of the $SrTiO_3$, $BaTiO_3$, $PbTiO_3$ and $CaTiO_3$ (011) surfaces are still rather large.

According to the results of my calculations for $SrTiO_3$ (111) surfaces, the upper layer Ti atom for Ti-terminated $SrTiO_3$ (111) surface strongly (by 3.58% of the bulk lattice constant a_0) relaxes inwards (see Table 8). The second layer Sr atom moves inwards by huge magnitude of 11.24% of a_0, while the second layer O atom relaxes outwards by 1.53% of a_0. Outward displacement of the third layer Ti atom is rather weak, less than 1% of a_0. For the SrO_3-terminated $SrTiO_3$ (111) surface the upper layer metal atom moves outwards by 1.33% of a_0, but the upper layer O atom is displaced very slightly inwards by 0.03% of a_0. The second layer Ti atom outward displacement (1.81% of a_0) is larger than the upper layer Sr atom outward relaxation. Both third layer Sr and O atoms relaxes inwards by a very small magnitude (0.03% of a_0 and 0.26% of a_0), respectively (see Table 8). The calculated surface relaxation energy for Ti-terminated $SrTiO_3$ (111) surface (−1.66 eV) is almost five times larger, than the surface relaxation energy for SrO_3-terminated $SrTiO_3$ (111) surface (−0.35 eV).

Ferroelectrics 2015.483:53-67.

Table 8

Calculated relaxation by means of the B3LYP method of Ti and SrO_3-terminated SrTiO3 (111), Ti and BaO_3-terminated $BaTiO_3$ and Ti and CaO_3-terminated $CaTiO_3$ (111) surface upper three layer atoms (as a percentage of the bulk crystal lattice constant $a_0 = 3.914$ Å, $a_0 = 4.021$ Å and $a_0 = 3.851$ Å, respectively)

$SrTiO_3$ (111) surface			$BaTiO_3$ (111) surface		$CaTiO_3$ (111) surface	
Layer	Ion	Δz	Ion	Δz	Ion	Δz
Ti-terminated $SrTiO_3$ (111) surface			Ti-term. BTO (111) surface		Ti-term. CTO (111) surface	
1	Ti	−3.58	Ti	−11.19	Ti	−6.23
2	Sr	−11.24	Ba	−6.22	Ca	−14.02
	O	1.53	O	+2.74	O	1.30
3	Ti	0.26	Ti	−0.25	Ti	−0.26
SrO_3-terminated $SrTiO_3$ (111) surface			BaO_3-term. BTO (111) surf.		CaO_3-term. CTO (111) surf.	
1	Sr	1.33	Ba	−1.24	Ca	−0.52
	O	−0.03	O	−3.98	O	−0.81
2	Ti	1.81	Ti	+2.49	Ti	+2.13
3	Sr	−0.03	Ba	+1.49	Ca	+2.60
	O	−0.26	O	−0.25	O	−0.07

According to the results of the calculations, the upper layer Ti atom for Ti-terminated $BaTiO_3$ (111) surface strongly (by 11.19% of the bulk lattice constant a_o) relaxes inwards (see Table 8). The second layer Ba atom also rather strongly relaxes inwards (by 6.22% of a_o), while the second layer O atom relaxes outwards by 2.74% of a_o. Inward relaxation of the third layer Ti atom is rather weak, only 0.25% of a_o. For BaO_3-terminated $BaTiO_3$ (111) surface the upper layer metal atom relaxes inwards by 1.24% of a_o, but the upper layer O atom relaxes inwards even more strongly by 3.98% of a_o (see Table 8). The second layer Ti atom outward relaxation (2.49% of a_o) is larger than upper layer metal - Ba atom relaxation. Third layer Ba atom rather strongly relax outwards, but third layer O atom relax inwards by a very small magnitude (0.25% of a_o).

Conclusions

According to all my calculations, on the AO-terminated (001) surface, all upper-layer A atoms relax inward for $SrTiO_3$, $BaTiO_3$, $PbTiO_3$ and $CaTiO_3$ perovskites by magnitude of at least 2% of the lattice constant a_0, while all second layer atoms relax outwards. For the TiO_2-terminated $SrTiO_3$, $BaTiO_3$, $PbTiO_3$ and $CaTiO_3$ (001) surface, in most cases, the largest relaxations are on the second-layer metal atoms. For almost all $SrTiO_3$, $BaTiO_3$, $PbTiO_3$ and $CaTiO_3$ perovskites, the (001) surface rumpling is much larger for the AO-terminated than for the TiO_2-terminated (001) surface, but their surface energies always are quite similar.

In contrast, according to my calculations, different terminations of the $SrTiO_3$, $BaTiO_3$, $PbTiO_3$ and $CaTiO_3$ (011) surface lead to very different surface energies for the O-terminated, A-terminated and TiO-terminated $SrTiO_3$, $BaTiO_3$, $PbTiO_3$ and $CaTiO_3$ (011) surface, respectively.

According to my calculations, the most energetically favourable with the lowest surface energy, always are the AO and TiO_2-terminated $SrTiO_3$, $BaTiO_3$, $PbTiO_3$ and $CaTiO_3$ perovskite (001) surfaces. The A, TiO and O-terminated $SrTiO_3$, $BaTiO_3$, $PbTiO_3$ and $CaTiO_3$ (011) surfaces are always, according to my calculations, less energetically favourable than the (001) surfaces. Finally, the $SrTiO_3$, $BaTiO_3$ and $CaTiO_3$ (111) surfaces are always energetically most unfavourable and unstable surfaces according to all my performed calculations.

The main reason for stability difference between (001), (011) and (111) surfaces stem from peculiarities of their atomic and electronic structure. Namely, the (001) cleavage of $SrTiO_3$, $BaTiO_3$, $PbTiO_3$ and $CaTiO_3$ gives rise to nonpolar (neutral) AO and TiO_2 (001) terminations, which are stable and have the lowest surface energy. A naive cleavage of $SrTiO_3$, $BaTiO_3$, $PbTiO_3$ and $CaTiO_3$ to create (011) or (111) surfaces leads to the formation of polar $SrTiO_3$, $BaTiO_3$, $PbTiO_3$ and $CaTiO_3$ (011) or (111) surfaces. The polar $SrTiO_3$, $BaTiO_3$, $PbTiO_3$ and $CaTiO_3$ (011) and (111) surfaces consists of alternating charged planes, and thereby they are energetically less stable than neutral (001) surfaces. Of course, the surface energies of polar $SrTiO_3$, $BaTiO_3$, $PbTiO_3$ and $CaTiO_3$ (011) and (111) surfaces are much larger than for the neutral (001) surfaces, in good agreement with the results of current *ab initio* calculations.

The current *ab initio* calculations indicate a considerable increase in the Ti-O chemical bond covalency near the TiO and O-terminated $SrTiO_3$, $BaTiO_3$, $PbTiO_3$ and $CaTiO_3$ (011) surfaces as well as the TiO_2-terminated (001) surface. The Ti-O chemical bond covalency at the TiO-terminated $SrTiO_3$, $BaTiO_3$, $PbTiO_3$ and $CaTiO_3$ (011) surface (0.130*e*, 0.130*e*, 0.132*e* and 0.128*e*, respectively) is much larger than that for the TiO_2-terminated (001) surface (0.118*e*, 0.126*e*, 0.114*e*, 0.114*e*, respectively) or in bulk

Ferroelectrics 2015.483:53-67.

(0.088*e*, 0.098*e*, 0.098*e*, 0.084*e*, respectively). The Ti-O chemical bond populations on the TiO-terminated $SrTiO_3$, $BaTiO_3$, $PbTiO_3$ and $CaTiO_3$ (011) surfaces are much larger in the direction perpendicular to the surface than in the plane (0.188*e*, 0.198*e*, 0.196*e*, 0.186*e* vs 0.130*e*, 0.130*e*, 0.132*e*, 0.128*e*, respectively). Performed *ab initio* calculations indicate also a considerable increase of Ti-O chemical bond covalency near the $SrTiO_3$, $BaTiO_3$, $PbTiO_3$ and $CaTiO_3$ (111) surface relative to the $SrTiO_3$, $BaTiO_3$, $PbTiO_3$ and $CaTiO_3$ bulk. This should have an impact on the electronic structure of surface defects (e. g. *F* centers), as well as on the adsorption and surface diffusion of atoms and small molecules relevant for catalysis.

Funding

This work was supported by the Latvian Council of Science Grant No. 374/2012 and ESF Grant No. 2013/0046/1DP/1.1.1.2.0/APIA/VIAA/021.

References

1. J. F. Scott, *Ferroelectric Memories*. Springer: Berlin; (2000).
2. M. Dawber, K. M. Rabe, and J. F. Scott, Physics of thin-film ferroelectric oxides. *Rev. Mod. Phys.* **77**, 1083–1130 (2005).
3. R. E. Cohen, Origin of ferroelectricity in perovskite oxides. *Nature*. **358**, 136–138 (1992).
4. W. Jia, V. S. Vikhnin, H. Liu, S. Kapphan, R. I. Eglitis, and D. Usvyat, Critical effects in optical response due to charge transfer vibronic excitons and their structure in perovskite-like systems. *Journal of Luminescence*. **83–84**, 109–113 (1999).
5. O. Auciello, J. F. Scott, and R. Ramesh, The Physics of Ferroelectric Memories. *Phys. Today*. **51**, 22–27 (1998).
6. J. A. Enterkin, A. K. Subramanian, B. C. Russel, M. R. Castell, K. R. Poeppelmeier, and L. D. Marks, A homologous series of structures on the surface of $SrTiO_3$ (110). *Nature Materials*. **9**, 245–248 (2010).
7. H. Tanaka, and T. Kawai, Surface structure of reduced $SrTiO_3$ (111) observed by scanning tunnelling microscopy. *Surf. Sci.* **365**, 437–442 (1996).
8. J. Chang, Y. S. Park, and S. K. Kim, Atomically flat single-terminated SrTiO3 (111) surface. *Appl. Phys. Lett.* **92**, 152910 (2008).
9. E. Blokhin, R. A. Evarestov, D. Gryaznov, E. A. Kotomin, and J. Maier, Theoretical modelling of antiferrodistortive phase transition for $SrTiO_3$ ultrathin films. *Phys. Rev. B.* **88**, 241407(R) (2013).
10. E. Heifets, R. I. Eglitis, E. A. Kotomin, J. Maier, and G. Borstel, *Ab initio* modeling of surface structure for $SrTiO_3$ perovskite crystals. *Phys. Rev. B.* **64**, 235417 (2001).
11. E. A. Kotomin, R. I. Eglitis, J. Maier, and E. Heifets, Calculations of the atomic and electronic structure for $SrTiO_3$ perovskite thin films. *Thin Solid Films.* **400**, 76–80 (2001).
12. S. Piskunov, E. A. Kotomin, E. Heifets, J. Maier, R. I. Eglitis, and G. Borstel, Hybrid DFT calculations of the atomic and electronic structure for ABO3 perovskite (001) surfaces. *Surf. Sci.* **575**, 75–88 (2005).
13. R. I. Eglitis, G. Borstel, E. Heifets, S. Piskunov, and E. Kotomin, *Ab initio* calculations of the $BaTiO_3$ (100) and (110) surfaces. *Journal of Electroceramics.* **16**, 289–292 (2006).
14. N. Erdman, K. R. Poeppelmeier, M. Asta, O. Warschkow, D. E. Ellis, and L. D. Marks, The structure and chemistry of the TiO_2-rich surface of $SrTiO_3$ (001). *Nature*. **419**, 55–57 (2002).
15. A. Hofer, M. Fechner, K. Duncker, M. Holzer, I. Mertig, and W. Widdra, Persistence of surface domain structures for a bulk ferroelectric above T-C. *Phys. Rev. Lett.* **108**, 087602 (2012).
16. R. I. Eglitis, and D. Vanderbilt, First-principles calculations of atomic and electronic structure of $SrTiO_3$ (001) and (011) surfaces. *Phys. Rev. B.* **77**, 195408 (2008).

Ferroelectrics 2015.483:53-67.

17. C. Bungaro, and K. M. Rabe, Coexistence of antiferrodistortive and ferroelectric distortions at the $PbTiO_3$ (001) surface. *Phys. Rev. B.* **71**, 035420 (2005).
18. R. I. Eglitis, and D. Vanderbilt, *Ab initio* calculations of the atomic and electronic structure of $CaTiO_3$ (001) and (011) surfaces. *Phys. Rev. B.* **78**, 155420 (2008).
19. A. M. Kolpak, D. Li, R. Shao, A. M. Rappe, and D. A. Bonnell, Evolution of the structure and thermodynamic stability of the $BaTiO_3$ (001) surface. *Phys. Rev. Lett.* **101**, 036102 (2008).
20. R. I. Eglitis, and D. Vanderbilt, *Ab initio* calculations of $BaTiO_3$ and $PbTiO_3$ (001) and (011) surface structures. *Phys. Rev. B.* **76**, 155439 (2007).
21. F. Bottin, F. Finocchi, C. Noguera, Stability and electronic structure of the (1×1) $SrTiO_3$ (110) polar surfaces by first-principles calculations. *Phys. Rev. B.* **68**, 035418 (2003).
22. C. Noguera, Polar oxide surfaces. *J. Phys.: Condens. Matter.* **12**, R367 (2000).
23. F. Bottin, F. Finocchi, and C. Noguera, *Ab initio* study of the polar $SrTiO_3$ (110) (1×1) surfaces. *Surf. Sci.* **532–535**, 468–471 (2003).
24. R. I. Eglitis, First-principles calculations of $BaZrO_3$ (001) and (011) surfaces. *J. Phys.: Condens. Matter.* **19**, 356004 (2007).
25. H. Chen, Y. Xie, G. H. Zhang, and H. T. Yu, A first-principles investigation of the stabilities and electronic properties of $SrZrO_3$ (110) (1×1) polar terminations. *J. Phys.: Condens. Matter.* **26**, 395002 (2014).
26. R. I. Eglitis, and M. Rohlfing, First-principles calculations of the atomic and electronic structure of $SrZrO_3$ and $PbZrO_3$ (001) and (011) surfaces. *J. Phys.: Condens. Matter.* **22**, 415901 (2010).
27. J. M. Zhang, J. Cui, K. W. Hu, V. Ji, and Z. Y. Man, *Ab initio* modelling of $CaTiO_3$ (110) polar surfaces. *Phys. Rev. B.* **76**, 115426 (2007).
28. N. Sivadas, H. Dixit, V. R. Cooper, and D. Xiao, Thickness-dependent carrier density at the surface of $SrTiO_3$ (111) slabs. *Phys. Rev. B.* **89**, 075303 (2014).
29. R. I. Eglitis, Ab initio calculations of $BaTiO_3$ (111) surfaces. *Phase Transitions.* **86**, 1115–1120 (2013).
30. W. Liu, C. Wang, J. Cui, and Z. Y. Man, Ab initio calculations of the CaTiO3 (111) polar surfaces. *Solid State Commun.* **149**, 1871–1876 (2009).
31. R. I. Eglitis, *Ab initio* calculations of the atomic and electronic structure of $BaZrO_3$ (111) surfaces. *Solid State Ionics.* **230**, 43–47 (2013).
32. R. I. Eglitis, First-principles calculations of the atomic and electronic structure of $CaTiO_3$ (111) surfaces. *Ferroelectrics.* **424**, 1–6 (2011).
33. S. Piskunov, E. Heifets, R. I. Eglitis, and G. Borstel, Bulk properties of $SrTiO_3$, $BaTiO_3$ and $PbTiO_3$ perovskites: an *ab initio* HF/DFT study. *Comput. Mater. Sci.* **29**, 165–180 (2004).
34. A. D. Becke, Density-functional thermochemistry. 3. The role of exact exchange. *J. Chem. Phys.* **98**, 5648–5652 (1993).
35. J. P. Perdew, and Y. Wang, Accurate and simple density functional for the electronic exchange energy: Generalized gradient approximation. *Phys. Rev. B.* **33**, 8800(R)-8802(R) (1986).
36. J. P. Perdew, and Y. Wang, Erratum: Accurate and simple density functional for the electronic exchange energy: Generalized gradient approximation. *Phys. Rev. B.* **40**, 3399(E)–3399(E) (1989).
37. J. P. Perdew, and Y. Wang, Accurate and simple analytic representation of the electron-gas correlation energy. *Phys. Rev. B.* **45**, 13244–13249 (1992).
38. H. J. Monkhorst, and J. D. Pack, Special points for Brillouin-zone integrations. *Phys. Rev. B.* **13**, 5188–5192 (1976).
39. V. R. Saunders, R. Dovesi, C. Roetti, M. Causa, N. M. Harrison, R. Orlando, and Zicovich-Wilson C. M., CRYSTAL-2006 User Manual. University of Torino. Torino, Italy; (2006).
40. A. Pojani, F. Finocchi, and C. Noguera, Polarity on the $SrTiO_3$ (111) and (110) surfaces. *Surf. Sci.* **442**, 179–198 (1999).
41. A. Pojani, F. Finocchi, and C. Noguera, A theoretical study of the unreconstructed polar (111) face of $SrTiO_3$. *Appl. Surf. Sci.* **142**, 177–181 (1999).

Ferroelectrics 2015.483:53-67.

42. K. H. Hellwege, and A. M. Hellwege, Ferroelectrics and Related Substances. *Landolt-Bornstein, New Series Vol. **3***. Springer: Berlin; (1969).
43. G. Shirane, R. Pepinsky, and B. C. Frazer, X-ray and Neutron Diffraction study of Ferroelectric $PbTiO_3$. *Acta Cryst.* **9**, 131–140 (1956).
44. B. J. Kennedy, C. J. Howard, and B. C. Chakoumakos, Phase transitions in perovskite at elevated temperatures –a powder neutron diffraction study. *J. Phys.: Condens. Matter.* **11**, 1479–1488 (1999).
45. N. Bickel, G. Schmidt, K. Heinz, and Müller K., Ferroelectric relaxation of the $SrTiO_3$ (100) surface. *Phys. Rev. Lett.* **62**, 2009–2012 (1989).
46. T. Hikita, T. Hanada, M. Kudo, and M. Kawai, Structure and electronic state of the TiO_2 and SrO terminated $SrTiO_3$ (100) surfaces. *Surf. Sci.* **287**, 377–381 (1993).

Ferroelectrics 2015.483:53-67.